BioGecko
ISSN: 2230-5807
Web of Science
Vol 05 Issue 01 2016

Silver Nanoparticle Therapy for Colon Cancer: A New Approach Using Honey Bee-Made Nanoparticles

Njabulo Ndebele,Andre Brink

Abstract

Biosynthesis of nanoparticles, which has recently been extensively studied, might have a wide range of biological uses, particularly in cancer treatment. Honey bee extract has been used to explain the new biosynthesis of silver nanoparticles (AgNPs) in this work. The biogenic AgNPs and the capping biomolecules of this work were also being investigated in vitro for their anti-colon cancer effects. X-ray diffraction (XRD), energy dispersive X-ray (EDX), scanning electron microscopy (SEM), and transmission electron microscopy were used to examine the biogenic AgNPs that were produced (TEM). Incorporating honey bee proteins, researchers discovered that the generated AgNPs had a spherical shape with a size range of 12 to 18 nm. It was found that AgNPs may be employed safely at 39 g/ml, based on the cytotoxicity findings of PBMCs on the AgNPs acquired. A 60 percent reduction in Bcl2 and survivin gene expression was seen when the biogenic AgNPs were tested against colon cancer growth in non-toxic doses. AgNPs and their capping biomolecules both show antiproliferative effects, with a preference for the naked AgNPs, but the capping biomolecules have a greater impact on cancer cell growth than the AgNPs alone.

Keywords: Cancer of the colon; AgNPs; Survivin; BCl2; honey bee

Introduction:

With nanomedicine, new therapeutic and diagnostic tools for humans are discovered via the use of precisely manufactured nanomaterials [1]. Nanotechnology and nanomedicine have collaborated to create a new trend in both therapeutic and pharmaceutical fields [2]. Recent years have seen a surge in interest in developing environmentally friendly nanotechnology that makes use of microbes and nanomaterials [3].
Reports [3-5] have shown the production of Au and

Ag nanoparticles using coriander leaf, henna leaf, and edible mushroom extracts. AgNPs may also be synthesized using other bee products, such as Mendoza-Reséndez [6]. (raw honey, royal jelly, honeydew honey and propolis). When it comes to commercialization and application, silver nanoparticles (AgNPs) offer the widest range of options these days [7]. The most promising nanoparticles in the realm of nanomedicine are AgNPs, which have antibacterial properties against a variety of microorganisms [1]. A major paucity of knowledge exists on the biological effects of AgNPs on human cells, however. Furthermore, there are just a few research on the anticancer properties of biogenic AgNPs. AgNPs' anti-proliferative effects on human glioma cells (U251) were recently reported in one of these experiments [2]. There is also evidence to suggest that AgNPs in the size range of 1-1000 nm might be very useful for cancer diagnostics and therapy, and as a result, a new field known as "nano-oncology" may emerge. There are many synthetic anticancer drugs, such as doxorubicin, that do not work as well as they should, so it is critical to develop new ones [9]. Honey bees may be used to synthesize AgNPs in a cost-effective and ecologically friendly manner. Synthesized AgNPs were also tested against human epithelial colorectaladen carcinoma for their molecular effect on gene expressions in cells.

You'll know exactly what you need and how to utilize it.

Silver nitrate (AgNO3) was purchased from SigmaAldrich. Cell culture media was provided by Lonza. Other chemicals were of analytical grade and used without any further purification

Gold nanoparticles may be synthesized using honey bee extract.

As many as fifty adult honey bee workers were taken from the SRTA-City Farm honey bee colony to be disinfected with 0.05 percent Clorox solution and three times sanitized with water. On a pre-sterilized laminar flow, the insects were allowed to dry completely. Sterile phosphate buffer (pH=7, 25 mM) was used to grind the insects after they had been washed with alcohol. This was followed by three layers of sterilized muslin filtering the extract into a 250-milliliter flask for each 100-milliliter portion. In the presence of glucose (560 Mm) as an electron donor, AgNO3 was added to the insect filtrate as a substrate for the formation of AgNPs. Stirring (220 rpm) was used to incubate the mixture at room temperature. A Shimadzu UV-Vis spectrophotometer was used to obtain 1.5 ml

samples from the reaction mixture at various times, and the resultant colloidal suspension of AgNPs was recorded instantly against the experimental blank at 450nm using Shimadzu UV-Vis. Centrifugation at 10,000 rpm for 20 minutes collected the AgNPs, which were then dissolved in 0.1 ml of 25 mM PBS at pH=7 and kept at 4°C until needed.

The production and characterization of AgNPs

Structural analysis of AgNP morphology has been carried out using a scanning electron microscope (JEOL SEM, GSM-6610LV, Japan) operating at fifteen thousand volts. For SEM, gold was vacuumcoated onto the samples' surfaces. X-ray diffraction (Shimadzu XRD 7000 X-ray diffractometer, Japan) and transmission electron microscopy (TEM) were used to characterize the produced AgNPs.

Cell cultivation is a term used to describe this procedure.

After two washes with DMEM media (Lonza) supplemented with 200 M L-glutamine and 25 mM HEPES buffer, CaCO2 (human epithelial colorectaladeno carcinoma, American Type Culture Collection, ATCC; Manassas, VA, USA) was used. In DMEM with 10% fetal bovine serum, 2 105 cells were cultured (Gibco-BRL). In an incubator (37°C, 5% CO2, 95% humidity), the cells were allowed to attach to the polystyrene 6-well plates for four hours. Using RPM1 supplemented medium, the cells were twice washed to remove debris and dead cells.

Separation of lymphocytes from human blood:

By using gradient centrifugation, Lohr et al. [10] separated peripheral blood cells mononuclear cells (PBMCs). To begin, we mixed 5 volumes of newly made RBC lysis buffer (38.8 mmol/L ammonium chloride, 2.5 mmol/L K2 HCO3, 1 mmol/L Ethylenediaminetetraacetic acid, pH 8.0), incubated at ambient temperature for 10 minutes, and centrifuged 1500 rpm for 5 minutes. Nucleated cells sank to their lowest point in the tube and remained there.

Proliferation and cytotoxicity tests:

In accordance with Borenfreund and Puerner [11], the safe dosage of the biogenic AgNPs was calculated using PBMC as a normal cell model. Six million cells/ml were planted into each of the 96well plates and incubated at 37°C with 5% CO2. About 100 l of various AgNPs concentrations were added after incubation. After three days of incubation, 100 l of neutral red stain solution (100 g /ml) was applied to both dead and live cells. A quantitative test was provided by the inclusion of neutral red stain into liposomes, which exclusively stained live cells. An automatic ELIZA microplate reader set to 540 nm measured the stain intensity. **Assessment of antiproliferative activity:**

The trypan blue test was used to validate the biogenic AgNPs' antiproliferative efficacy on CaCO2 cells. There are live cells in a cell suspension when the dye exclusion test is performed. Because the trypan blue stain may be used to evaluate cell membrane integrity, it can be used to determine whether or not cells are growing or dying. 5Fluorouracil (5 FU, 0.9 g/ml) or biogenic AgNPs (39g/ml) were administered to CaCO2 cells for 48 hours without causing any harm to the cells. In order to test whether or not cells absorb or reject dye, the suspensions of treated cells were simply combined with dye and then visually evaluated to compare to untreated cells as a control at the conclusion of incubation. A blue cytoplasm indicates the presence of dead cells in this technique, while the transparent cytoplasm indicates the presence of live cells.

The biogenic AgNPs' anticancer properties: Target gene repression mechanisms:

Synthesized biogenic AgNPs' anticancer activity profile was explained by looking at how they affected gene expression in CaCO2 cells for p53, Bcl2, caspase 3, and survivin. Both biogenic AgNPs and 5FU were added to the growth medium of 6x103 CaCO2 cells/ml in 12 well plates for two days (as a positive control). RT-q PCR was used to compare the expression levels of genes before and after therapy after extracting total cellular RNA. In order to synthesis the first-strand cDNA, the oligo-dT primer and the AMV reverse transcriptase (Promega Corp., Madison, WI) were utilized. When doing PCR product standardization, GAPDH was employed as an internal control. This was done using the SYBR Green dye and a Light Cycler fluorimeter on the cDNA (BIO RAD S1000 Tm thermal cycler, supplied by Quantitect SYBR Green PCR Kits) (Table 1). Identifying the biomolecules that encase the AgNPs: There were three extractions using three litres of 100% ethanol, three times, of potential biomolecules responsible for capping the produced AgNPs, to summarize. Extraction proceeded overnight at a temperature of 4°C. Centrifugation at 40,000 rpm for ten minutes yielded

the produced pellet. Following a PBS wash, an FTIR analysis was performed to determine the identity of the pellet and compare it to that of the full particles. As previously noted, ethanol precipitation was used to separate the bio-synthesized AgNPs from their capping biomolecules, in order to study the potential anticancer effects of these compounds in combination. AgNPs or capping biomolecules were applied to a semi-confluent layer of CaCO2 cells for 48 hours. Trypan blue dye was used to evaluate cellular viability at the conclusion of incubation, as reported before.

Results and Discussion:

The produced AgNPs were subjected to UV-Vis spectral analysis.

The color change in the reaction mixture (AgNO3 solution + honey bee extract) was used to validate the synthesis of AgNPs, which is due to the reduction of Ag+ ions into Ag atoms and subsequently into nanoparticles by the reaction. In addition, the absorbance of AgNPs colloidal suspension was measured at 450 nm, as previously described in the technique section.

Primers	Sequence
Bcl2-forward	5'-TATAAGCTGTCGCAGAGGGGCTA3'
Bcl2-reverse	5'-GTACTCAGTCATCCACAGGGCGAT3'
P53-forward	5'-AACGGTACTCCGCCACC-3'
P53-reverse	5'-CGTGTCACCGTCGTGGA-3'
Caspase-3-forward	5'-TGCGCTGCTCTGCCTTCT-3'
Caspase-3-reverse	5'-CCATGGGTAGCAGCTCCTTC-3'
Survivin-forward	5'-TGCCCCGACGTTGCC-3
Survivin-reverse	5'-CAGTTCTTGAATGTAGAGATGCGGT-3'
GAPDH-forward	5'-GAA GGT GAA GGT CGG AGT
GAPDH-reverse	3'-GAA GAT GGT GAT GGG ATT TC

Table 1: List of primers.

	Day 1	Day 2	Day 3	Day 4	Day 5
OD (450 nm)	0.561	0.822	0.856	0.896	0.891

Table 2: UV-Vis spectral analysis of the biosynthesis of AgNPs.

An explanation for this absorption is that nanoparticles have a surface plasmon resonance (SPR). Table 2 shows the UV-vis absorption corresponding to the bio reduction of Ag+ ions in aqueous solution at various time periods. AgNP biosynthesis was almost complete after four days of incubation, according to the findings of this study.

AgNPs: chemical and physical characterization

EDX analysis findings and a scanning electron micrograph of the honey bee-prepared AgNPs are displayed in Figure 1I. Using raw honey bee extract, it is clear that the AgNPs produced are spherical. SEM-EDX was used to conduct the elemental analysis of the honey bee-produced AgNPs, as shown in Figure 1II. Results indicated that the main components of the resultant AgNPs were carbon, oxygen, and silver. It has been confirmed by EDX quantitative analysis that the nanostructure of the AgNPs is composed of around 19.85 wt% Ag, 45.22 wt% carbon, and about 34.93 wt% oxygen. The XR diffractogram of the biosynthesized AgNPs is shown in Figure 2. The crystalline nature of the AgNPs, as seen in the image, confirms that they are made of elemental Ag (0). In addition, the calculated size of the generated AgNPs varied from 20 to 60 nm, based on the experiment. (111), (201) and (311) are the three planes that show in the diffraction peaks at 32.3, 46.6 and 76.8 correspondingly.

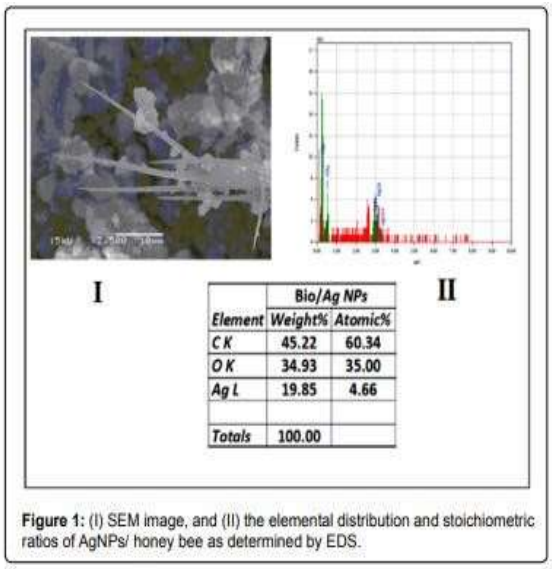

Figure 1: (I) SEM image, and (II) the elemental distribution and stoichiometric ratios of AgNPs/ honey bee as determined by EDS.

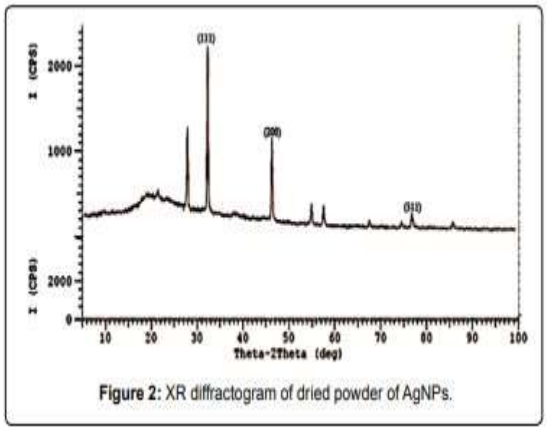

Figure 2: XR diffractogram of dried powder of AgNPs.

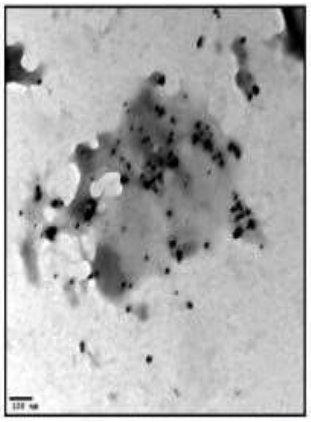

Figure 3: TEM micrographs of the AgNPs capped with the honey bee biomolecules.

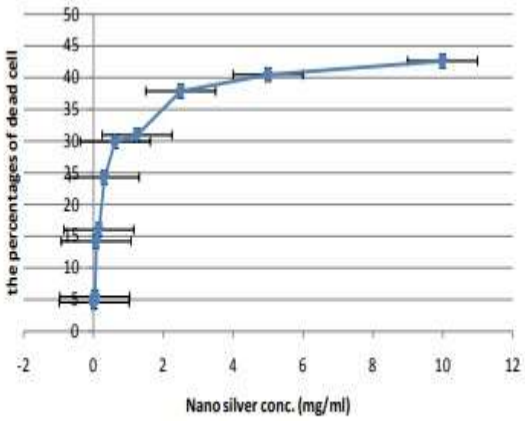

Figure 4: Cytotoxicity assay of the developed biogenic AgNPs on peripheral blood mononuclear cells.

bee

Figure 3 shows the TEM images of the surface morphology of the generated AgNPs. The AgNPs can be seen in the image to be dense and spherical, ranging in size from 12 to 18 nm. The produced AgNPs are implanted on the honey biomolecules, as seen by the TEM micrograph.

Cytotoxicity assay of the biogenic AgNPs

PBMC cytotoxicity testing was used as a benchmark for the therapies' safety in humans since it was easy to conduct. According to the cytotoxicity data presented in Figure 4, a dose of 39 g/ml of biogenic

Assessment of the antiproliferative activity

Fig. 5 shows the anti-proliferative action of biogenic AgNPs on CaCO2 cells AgNPs interaction with CaCO2 cells resulted in a 60% decrease of cellular viability, compared to 66.68% in cells treated with 5 FU, according to the data.

Target	Sample	Mean Cq	Mean Efficiency Corrected Cq	Normalized Expression	Relative Normalized Expression	Regulation	Compared to Regulation Threshold
bcl2	5 Fu	28.36	28.36	1.61248	0.07412	13.49113	Down regulated
bcl2	(-ve) Control	28.86	28.88	21.75417	1	1	No change
bcl2	AgNPs	32.44	32.44	0.46529	0.02139	46.75447	Down regulated
caspase 3	5 Fu	N/A	N/A	N/A	N/A	N/A	No change
caspase 3	(-ve) Control	N/A	N/A	N/A	N/A	N/A	No change
caspase 3	AgNPs	N/A	N/A	N/A	N/A	N/A	No change
GAPDH	5 Fu	20.05	20.05	N/A	N/A	N/A	No change
GAPDH	Control	20.3	20.3	N/A	N/A	N/A	No change
GAPDH	AgNPs	21.34	21.34	N/A	N/A	N/A	No change
p53	5 Fu	23.51	23.51	10.16548	0.94442	2.94442	No change
p53	(-ve) Control	27.79	27.79	45.57888	1	1	No change
p53	AgNPs	27.36	27.36	15.80025	0.34666	2.88489	No change
Survivin	5 Fu	27.53	27.53	8.79725	0.03707	26.97448	Down regulated
Survivin	(-ve) Control	26.02	26.02	155.2568	1	1	No change
Survivin	AgNPs	34.17	34.17	0.14004	0.0009	1108.63206	Down regulated

Table 2: Gene expression regulation via the biogenic AgNPs treatment.

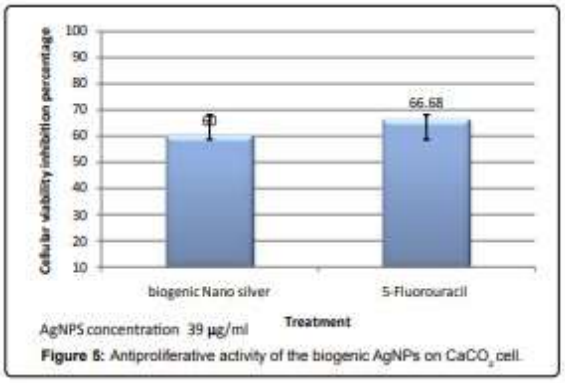

Figure 5: Antiproliferative activity of the biogenic AgNPs on $CaCO_2$ cell.

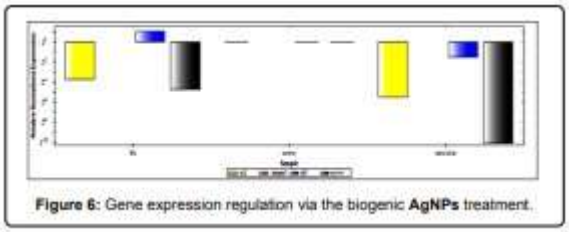

Figure 6: Gene expression regulation via the biogenic **AgNPs** treatment.

AgNPs with a cellular viability inhibition percentage of 5.453 is the most suggested dosage. However, the non-toxic dosage of 5-Fluorouracil (5 FU) as a positive control has reached 0.9 g/ml, with an inhibition percentage of 10.9 percent (Data is not shown). According to this study, 5 FU was shown to be more harmful for PBMC than the biogenic AgNPs that were created by researchers at the National Cancer Institute.

The mechanisms of gene regulation targeted by the biogenic AgNPs:

Gene expression patterns have been used to study the potential processes by which AgNPs cause cell death through the apoptotic regulators. Figure 6 shows the results of quantitative RT-PCR with GAPDH expression normalization used to examine the apoptotic pathway to determine RNA levels of Bcl2, survivin, and caspase3. In addition, the effects of AgNPs on gene expression were compared to those of 5 FU, a typical anticancer medication.

Conclusions from this study show that AgNPs administration may promote cell death in human epithelial colorectaladeno carcinoma cells by downregulating the expression of both survivin and bcl2 genes, although caspase3 expression is unaffected. Treatment with 5 FU also reduces Bcl2 and survivin gene expression, albeit at lower regulatory levels than treatment with AgNPs (Table 3).

FTIR analysis of the AgNPs capping biomolecules

Figure 7a shows the FTIR spectrum of the AgNPs extracted from biomolecules. The pure biomolecule frequencies are shown as follows: More specifically, the C-O-C asymmetric stretching and bending vibrations are responsible for 3446 cm1 and the CNH group stretching vibration is responsible for 1097 cm1. The hydrogen-bonded OH stretching vibrations are responsible for the bands at 2467 cm1 and 841 cm1. But as seen in Figure 7b, a big peak at 3510 cm1 in AgNPs with their encapsulated biomolecules indicates that a high quantity of carbohydrates is present, as demonstrated by the N–H stretch band merging with this hydroxyl peak. CH stretching vibrations may be identified by the strong absorption peaks at 2890 cm1 and the strong absorption peaks at 1652–1656 cm1 and the band at 1423 cm1, which is suggestive of C-C stretching, respectively (corresponding to carbohydrates linked with AgNPs). -CC-stretching in carbs has been shown to be linked to AgNPs absorbance at 2165 cm-1, which is an indicator of the presence of carbohydrates.

Anticancer activities of the AgNPs and their capping biomolecules:

Anticancer activities of both AgNPs and their capping biomolecules were evaluated as shown in Figure 8 to determine which portion of the biogenic AgNPs was responsible for the anti-proliferative activity against CaCO2 cells. Both AgNPs and their capping biomolecules displayed anti-proliferative activities against colon cancer superior to the 58.6 percent inhibition of the naked AgNPs, as seen in the figure With their biomolecules, the capping biomolecules exhibited 60% inhibition, but the AgNPs with their biomolecules showed 57% inhibition. Simple, large-scale commercial manufacturing and medicinal applications are possible with the green and eco-friendly method to synthesis of AgNPs. Honey and other bee products have long been utilized as medicinal agents because of their unique health advantages, including antibacterial, antioxidant, anticancer, antiinflammatory, and anti-inflammatory properties.

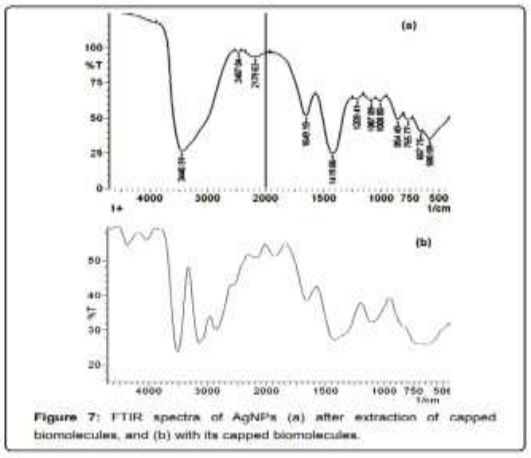

Figure 7: FTIR spectra of AgNPs (a) after extraction of capped biomolecules, and (b) with its capped biomolecules.

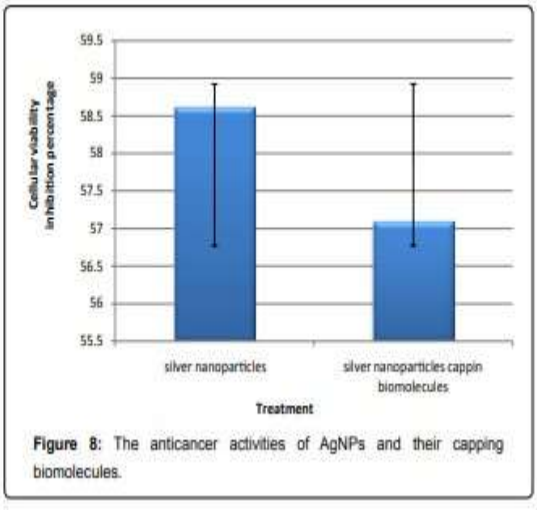

Figure 8: The anticancer activities of AgNPs and their capping biomolecules.

antiviral AgNP biosynthesis employing honey bee workers was accomplished within a few days, with

particle sizes ranging from 12 to 18 nm, in the present research. According to the results of the EDX study, the Ag ions in the honey bee biomolecules were well-prepared and had not undergone any chemical or structural alterations. There are 32.3°, 46.6°, and 76.8° points on the XRD spectrum that correspond to the facets of an X-ray diffraction-detected cubic crystal with facets (111), (200), and (311). The green manufacturing of nanoparticles is still a mystery. It has recently been revealed that biomolecules such as protein and flavonoids present in the bio-systems have a significant role in the reduction of metal ions and in capping nanoparticles [16]. After comparing results from Murugaraj [17] with the present findings, it is obvious that a portion of honey bee biomolecules was associated with AgNPs through free amino groups and/or carboxylic acids. They were not only responsible for the reduction of Ag+ into Ago, but they also worked as stabilizing capping agents for Ago and may also increase the biological characteristics of the produced AgNPs. The amino groups were shown to be the primary agents in the reduction of Ag+ ions and highly adsorbable to them. A decreased agglomeration propensity and increased stability of the produced AgNPs were also shown by SEM micrographs. Biogenic nanoparticles might be employed in cancer therapy as an alternative or complimentary agent because of their ability to interact with biomolecules and noble metals. The non-toxic dosage of AgNPs for PBMC was 39 g/ml in this investigation. CaCo2 cell growth was 60% inhibited by this dosage. CaCO2 cells are the focus of this information. The treatment of 50 g/ml AgNP concentrations resulted in 100% cell death in MCF7 and other human cancer cells [18]. It has been shown that AgNPs produced from mushrooms may be very hazardous to MDA-MB-231 cell lines, even at low concentrations of about 6 g/ml. [19] Nanoparticle cytotoxicity seems to be highly dependent on cell type and nanoparticle size, as shown by these results. When nanoparticles enter the body, reactive oxygen species (ROS) are generated, resulting in oxidative stress. Proteins and DNA are among the intracellular macromolecules with which inorganic nanoparticles interact significantly in cells. Nanoparticles' interaction with DNA is still a mystery [21]. Gene expression regulation-based apoptosis-inducing drugs might be created as novel anti-tumor medicines without triggering an inflammatory response. Survivin and bcl2 overexpression in colorectal cancer is strongly linked to p53 in a p53-independent way in this research. In neuroblastoma [22], gastric cancer [23], and breast cancer [24], a similar connection between survivin and bcl-2 was found. Survivin expression and p53 alterations in colorectal cancer were not linked, as they were in gastric cancer [23]. TATAfree and GC-rich promoter sequences govern the expression of both survivin and bcl-2 genes [25]. No matter how they co-express, survivin and bcl-2 have distinct anti-apoptosis mechanisms that do not overlap. The abundance of survivin in altered cell types and a wide range of human malignancies in vivo, however, was not detected in adult tissues like bcl2 [25].

Conclusion:

Honey bee extract was used as a new reducing agent in this work to manufacture biogenic AgNPs with a size range of 12-18 nm. In comparison to 5 FU, the synthesized AgNPs and the biomolecules that capped them displayed anti-colon cancer activity on the cellular and molecular levels. AgNPs manufactured in a single step using renewable resources may be useful in the treatment of colon cancer or for medication delivery.

Acknowledgement:

As a researcher at the Plant Protection and Biomolecular Diagnostics Department, Arid Lands Cultivation Research Institute in the City of Scientific Research and Technology Applications in Egypt, we would like to express our gratitude to Dr. Saad El Masry.

References

1.Sriram MI, Barath S, Kanth M, Kalishwaralal K, Gurunathan S (2010) Antitumor activity of silver nanoparticles in Dalton's lymphoma ascites tumor model. Int J Nanomed 5: 753-762

2. Asha Rani PV, Prakash Hande M, Valiyaveettil S (2009) Anti-proliferative activity of silver nanoparticles. BMC Cell Biology 10:65. 3. Kasthuri J, Kathiravan K, Rajendiran N (2009) Phyllanthin-assisted biosynthesis of silver and gold nanoparticles: a novel biological approach. J Nanopart Res 11: 1075.

4. Sathishkumar M, Sneha K, Won SW, Cho CW, Kim S, et al. (2009) Cinnamon zeylanicum bark extract and powder mediated green synthesis of nanocrystalline silver particles and its bactericidal activity. Colloid Surf.B 73: 332- 338.

5. Philip D (2009) Biosynthesis of Au, Ag and AuAg nanoparticles using edible mushroom extract. SpectrochimActa A 73: 374-381.

6. Mendoza-Reséndez R, nunez NO, and Luna C (2012) Green Synthesis of Silver Nanoparticles Mediated by Bee Products, 13 th

edition of trends in nanotechnology international conferecnce.
7. Ahmed M, Karns M, M. Goodson J, Rowe S, Hussain et al. (2008) DNA damage response to different surface chemistry of silver nanoparticles in mammalian cells. Toxicology and Applied Pharmacology 233: 404.
8. Yezhelyev MV, Gao X, Xing Y, Al-Hajj A, Nie S (2006) Emerging use of nanoparticles in diagnosis and treatment of breast cancer. Lancet Oncol: 657- 667.
9. Kim E, Kuk K, Yu J, Kim S, Park H, et al. (2007) Antimicrobial effects of silver nanoparticles. Nanomedicine: 3-95.
10. Lohr HF, Goergen B, Meyer zumBuschenfelde KH, Gerken G (1995) HCV replication in mononuclear cells stimulates anti-HCV-secreting B cells and reflects nonresponsiveness to interferonalpha. J Med Virol 46: 314-20.
11. Borenfreund E, Puerner JA (1985) Toxicity determined in vitro by morphological alterations and neutral red absorption. J Toxicol Lett 24: 119-124. 12. Nanji A, Zhao S, Sadrzadeh S, Waxman D (1994) Use of reverse transcriptasePCR to evaluate in vivo cytokine gene expression in chronic ethanolfed rats. Hepatology 19: 1483-1487.
13. Viuda-Martos M, Ruiz-Navajas Y, Fernlndezoopez, Pérez-llvarez (2008) Functional properties of honey, propolis, and royal jelly. Journal of Food Science 73: R117.
14. Narayanan K, Sakthivel (2008) Coriander leaf mediated biosynthesis of gold nanoparticlesMater. Lett 62: 4588-4590.
15. Huang J, Li Q, Sun D, Lu Y, Su Y (2007) Biosynthesis of silver and gold nanoparticles by novel sundried Cinnamomum camphora leaf. Chen, Nanotechnology 18: 105104-105114.
16. Vedpriya A (2010) living systems: eco-friendly nanofactories. Dig J Nanomater Bios 5: 9-21 17.Murugaraj J, Manoharan R, Renganathan A, Davoodbasha M, Gnanasekar S, et al. (2013) An Investigation on the cytotoxicity and caspasemediated apoptotic of biologically synthesized silver nanoparticles using Podophyllumhexandrum on human cervicalcarcinomacells effect. Colloids and Surfaces B: Biointerfaces102 : 708- 717. 18. Jeyaraj M, Sathishkumar G, Sivanandhan G, Mubarak Ali D, Rajesh M, et al. (2013) Biogenic silver nanoparticles for cancer treatment: an experimental report. Colloids Surf B 106: 86-92. 19. Gurunathan S, Jegadeesh R, Sri Nurestri AM, Priscilla AJ, Vikineswary S (2013) Green synthesis of silver nanoparticles using Ganoderma neojaponicumImazeki: a potential cytotoxic agent against breast cancer cellsInt. J. Nanomedicine 8: 4399-4413.
20. Park MVDZ, Neigh AM, Vermeulen JP (2011) The effect of particle size on the cytotoxicity, inflammation, developmental toxicity and genotoxicity of silver nanoparticles. Biomaterials 32: 9810-9817.
21. Molina MAF, Gamboa EM, Rivera CAS, Flores RAG, Zapata-Benavides P, et al. (2010) Antitumor activity of colloidal silver on MCF-7 human breast cancer cells. Padilla J Exp Clin Cancer Res 29: 148.
22. Adida C, Berrebi D, Peuchmaur M, ReyesMugica M, Altieri DC (1998) Antiapoptosisgene, survivin and prognosis of neuroblastoma. Lancet 351: 882- 883.
23. Lu CD, Altieri DC, Tanigawa N (1998)
Expression of a novel antiapoptosis gene, surviving, correlated with tumor cell apoptosis and p53 accumulation in gastric carcinomas. Cancer Res 58: 1808-1812.
24. Keitaro T, Shinji I, Goki G (2000) Expression of survivin and Its Relationship to Loss of Apoptosis in Breast Carcinomas. Clin Cancer Res 6: 127-134.
25. Ambrosini G, Adida C, Altieri DC (1997) A novel anti-apoptosis gene, survivin, expressed in cancer and lymphoma. Nat Med: 917-921.